Acta Cryst E CRYSTALLOGRAPHIC COMMUNICATIONS

ISSN 2056-9890

Crystal structure and Hirshfeld surface analysis of hexyl 1-hexyl-2-oxo-1,2-dihydroquinoline-4-carboxylate

Younos Bouzian,[a]* Sevgi Kansiz,[b]* Lhassane Mahi,[c] Noureddine Hamou Ahabchane,[a] Joel T. Mague,[d] Necmi Dege,[e] Khalid Karrouchi[f] and El Mokhtar Essassi[a]

[a]Laboratory of Heterocyclic Organic Chemistry URAC 21, Pole of Competence Pharmacochemistry, Av Ibn Battouta, BP 1014, Faculty of Sciences, Mohammed V University, Rabat, Morocco, [b]Department of Fundamental Sciences, Faculty of Engineering, Samsun University, Samsun 55420, Turkey, [c]Moroccan Foundation for Advanced Science Innovation and Research (Mascir), Department of Nanotechnology, Rabat Design Center, Rue Mohamed Al Jazouli-Madinat Al Irfane, Rabat 10 100, Morocco, [d]Department of Chemistry, Tulane University, New Orleans, LA 70118, USA, [e]Department of Physics, Faculty of Arts and Sciences, Ondokuz Mayıs University, Samsun, 55200, Turkey, and [f]Laboratory of Analytical Chemistry and Bromatology, Faculty of Medicine and Pharmacy, Mohamed V University, Rabat, Morocco.
*Correspondence e-mail: younos.bouzian19@gmail.com, sevgi.kansiz85@gmail.com

Received 24 February 2020
Accepted 1 April 2020

Edited by M. Weil, Vienna University of Technology, Austria

Keywords: crystal structure; dihydroquinoline; aliphatic chains; π-stacking; Hirshfeld surface analysis.

CCDC reference: 1994187

Supporting information: this article has supporting information at journals.iucr.org/e

The asymmetric unit of the title compound, $C_{22}H_{31}NO_3$, comprises of one molecule. The molecule is not planar, with the carboxylate ester group inclined by 33.47 (4)° to the heterocyclic ring. Individual molecules are linked by $_{aromatic}C—H\cdots O_{carbonyl}$ hydrogen bonds into chains running parallel to [001]. Slipped π–π stacking interactions between quinoline moieties link these chains into layers extending parallel to (100). Hirshfeld surface analysis, two-dimensional fingerprint plots and molecular electrostatic potential surfaces were used to quantify the intermolecular interactions present in the crystal, indicating that the most important contributions for the crystal packing are from H···H (72%), O···H/H···O (14.5%) and C···H/H···C (5.6%) interactions.

1. Chemical context

Quinoline derivatives represent an important class of heterocyclic compounds utilized as pharmaceuticals (Chu *et al.*, 2019). They possess various biological properties such as antibacterial (Panda *et al.*, 2015), anticancer (Tang *et al.*, 2018), antitubercular (Xu *et al.*, 2017), antiviral (Sekgota *et al.*, 2017), anti-HCV (Cannalire *et al.*, 2016), antimalarial (Hu *et al.*, 2017), anti-Alzheimer's (Bolognesi *et al.*, 2007), anti-leishmanial (Palit *et al.*, 2009) and anti-inflammatory (Pinz *et al.*, 2016) activities.

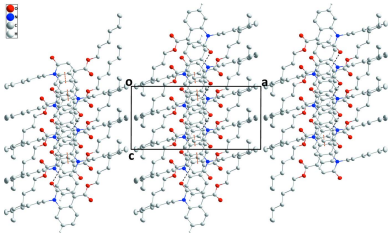

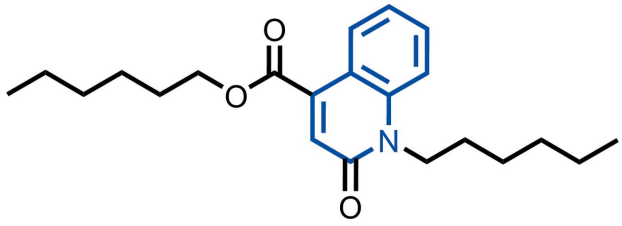

In view of the biological importance of quinoline, and in a continuation of our research work devoted to the syntheses and crystal structures of quinoline derivatives (Bouzian *et al.*, 2019*a*,*b*), we report herein on the molecular and crystal structures of hexyl 1-hexyl-2-oxo-1,2-dihydroquinoline-4-carboxylate, (I), which was prepared by reacting ethyl 6-chloro-2-oxo-1,2-dihydroquinoline-4-carboxylate with

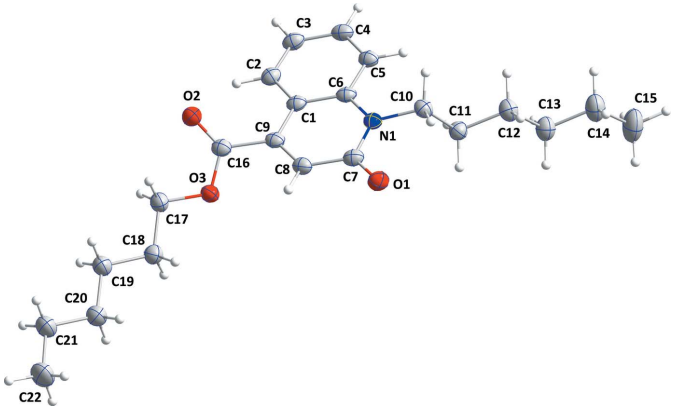

Figure 1
The title molecule with displacement ellipsoids drawn at the 50% probability level.

1-bromohexane in the presence of a catalytic quantity of tetra-*n*-butylammonium bromide. Intermolecular interactions were quantified by Hirshfeld surface analysis.

2. Structural commentary

The molecule of (I) is shown in Fig. 1. It is non-planar, with the carboxyl ester group inclined by 33.47 (4)° to the heterocyclic ring (r.m.s. deviation of the ten atoms = 0.0174 Å). The hexyl chain attached to N1 is twisted out of this plane by 14.2 (2)° whereas the hexyl chain attached to O1 is twisted by 23.1 (2)° from this plane.

3. Supramolecular features

In the crystal, C4—H4···O1 hydrogen bonds between the phenyl ring and the carbonyl group of an adjacent molecule lead to the formation of chains running parallel to [001] (Table 1, Fig. 2). These chains are connected in pairs along [010] through slipped π–π stacking interactions between

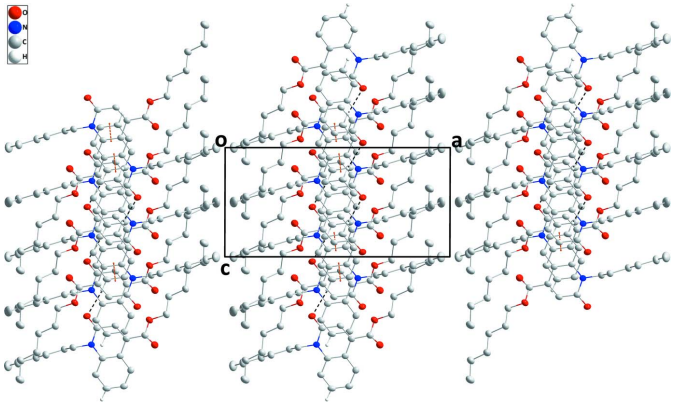

Figure 2
The crystal packing viewed along [010], with C—H···O hydrogen bonds and π–π stacking interactions indicated by black and orange dashed lines, respectively.

Table 1
Hydrogen-bond geometry (Å, °).

D—H···A	D—H	H···A	D···A	D—H···A
C4—H4···O1^{i}	0.960 (17)	2.475 (17)	3.3670 (19)	154.7 (15)

Symmetry code: (i) $x, y, z+1$.

inversion-related dihydroquinoline moieties [$Cg1\cdots Cg2^{i}$ = 3.5472 (9) Å with a slippage of 0.957 Å; $Cg1$ and $Cg2$ are the centroids of the N1/C6/C1/C9/C8/C7 and C1–C6 rings; symmetry code: (i) $1-x, -y, 1-z$] (Figs. 2, 3). This way, (100) layers with a width corresponding to the length of the a axis are formed. Unlike the packing features of similar molecules, the hexyl chains are not oriented in parallel. This is possibly a consequence of the π–π stacking interactions, which result in a 'crossed' orientation of neighbouring hexyl groups (Fig. 3).

4. Database survey

A search of the Cambridge Structural Database (CSD, version 5.40, update of August 2019; Groom *et al.*, 2016) using 2-oxo-1,2-dihydroquinoline-4-carboxylic acid as the main skeleton revealed five structures similar to the title compound. They contain the oxoquinoline moiety with different substituents, *viz*. 2-oxo-1,2-dihydroquinoline-4-carboxylic acid monohydrate (EQAVAV; Filali Baba *et al.*, 2016), ethyl 1*H*-3-hydroxy-2-oxo-1,2-dihydroquinoline-4-carboxylate (RAVJAA01; Paterna *et al.*, 2013), ethyl 1-methyl-2-oxo-1,2-dihydroquinoline-4-carboxylate (SECCAH; Filali Baba *et al.*, 2017*a*), prop-2-yn-1-yl 2-oxo-1-(prop-2-yn-1-yl)-1,2-dihydroquinoline-4-carboxylate (XILYUP; Filali Baba *et al.*, 2017*b*) and ethyl 1-benzyl-3-hydroxy-2-oxo-1,2-dihydroquinoline-4-carboxylate (ZINHEL; Paterna *et al.*, 2013). The layers present in EQAVAV are linked together by pairwise N—H···O interactions. In SECCAH, weak C—H···O hydrogen bonds link the molecules into zigzag chains along [100]. A single weak C—H···O intermolecular interaction links the molecules into [001] chains in XILYUP.

5. Hirshfeld surface analysis

To investigate the intermolecular interactions, Hirshfeld surface analysis (Spackman & Jayatilaka, 2009) and two-dimensional fingerprint plots were generated for the molecule using *CrystalExplorer17.5* (Turner *et al.*, 2017). Hirshfeld surface analysis depicts intermolecular interactions by

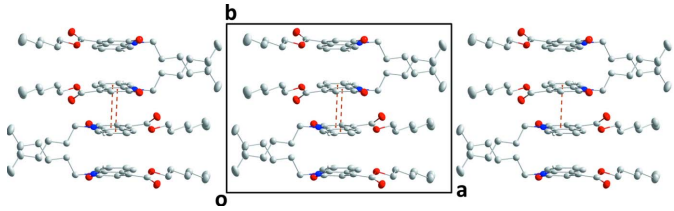

Figure 3
The crystal packing viewed along [001], with π–π stacking interactions indicated by orange dashed lines.

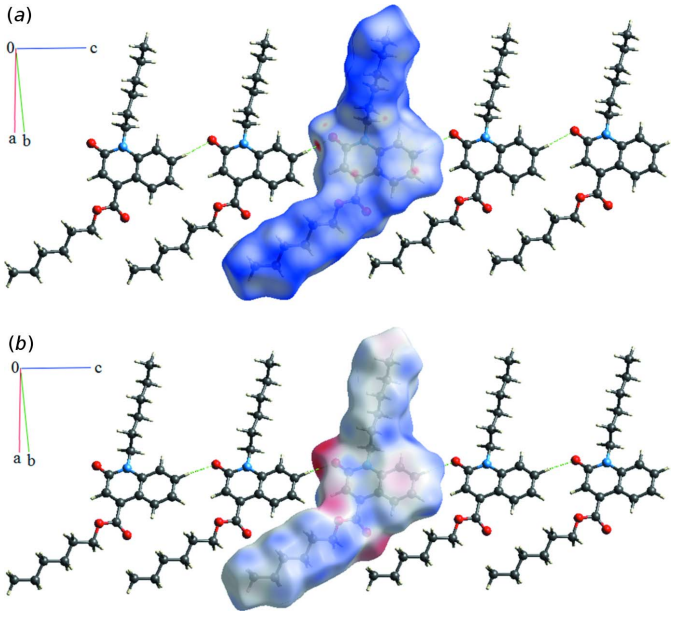

Figure 4
(*a*) The Hirshfeld surfaces of the title compound mapped over d_{norm}, with a fixed colour scale of −0.1822 (red) to 1.3083 (blue) a.u., and (*b*) the Hirshfeld surface mapped over molecular electrostatic potential showing C—H···O hydrogen bonds, with a fixed colour scale of −0.0733 (red) to 0.0381(blue) a.u..

different colours, representing short or long contacts and further the relative strength of the interaction. The generated Hirshfeld surface mapped over d_{norm} is shown in Fig. 4*a*. A view of the three-dimensional Hirshfeld surface of the title compound plotted over electrostatic potential, highlighting the C—H···O contacts, is given in Fig. 4*b*. As revealed by the two-dimensional fingerprint plots (Fig. 5), the crystal packing is dominated by H···H contacts, representing van der Waals interactions (72% contribution to the overall surface), followed by O···H and C···H interactions, which contribute with 14.5% and 5.6%, respectively. The contributions of the C···C (5.4%), C···O (0.8%), C···N (0.7%) and N···H (0.6%) interactions are less significant.

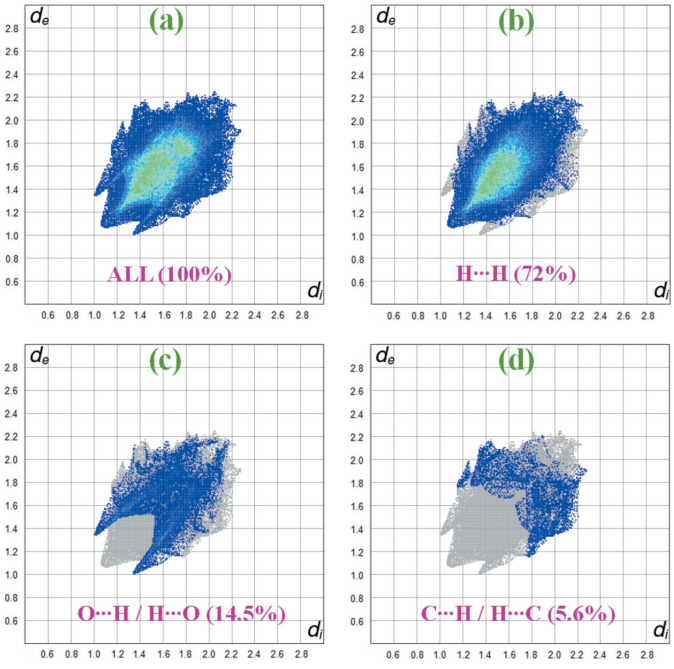

Figure 5
Two-dimensional fingerprint plots to the Hirshfeld surface with (*a*) a d_{norm} view for (I) and delineated into relative contributions for (*b*) H···H, (*c*) O···H/H···H and (*d*) C···H/H···C interactions.

Table 2
Experimental details.

Crystal data	
Chemical formula	$C_{22}H_{31}NO_3$
M_r	357.48
Crystal system, space group	Monoclinic, $P2_1/c$
Temperature (K)	150
a, b, c (Å)	17.6928 (7), 13.2512 (5), 8.5916 (3)
β (°)	90.184 (2)
V (Å^3)	2014.30 (13)
Z	4
Radiation type	Cu $K\alpha$
μ (mm^{-1})	0.61
Crystal size (mm)	0.25 × 0.17 × 0.10
Data collection	
Diffractometer	Bruker D8 VENTURE PHOTON 100 CMOS
Absorption correction	Multi-scan (*SADABS*; Krause *et al.*, 2015)
T_{min}, T_{max}	0.82, 0.94
No. of measured, independent and observed [$I > 2\sigma(I)$] reflections	14697, 3924, 3044
R_{int}	0.048
(sin $\theta/\lambda)_{max}$ (Å^{-1})	0.618
Refinement	
$R[F^2 > 2\sigma(F^2)]$, $wR(F^2)$, S	0.046, 0.105, 1.07
No. of reflections	3924
No. of parameters	359
H-atom treatment	All H-atom parameters refined
$\Delta\rho_{max}$, $\Delta\rho_{min}$ (e Å^{-3})	0.19, −0.18

Computer programs: *APEX3* and *SAINT* (Bruker, 2016), *SHELXT/5* (Sheldrick, 2015*a*), *SHELXL2018/3* (Sheldrick, 2015*b*), *DIAMOND* (Brandenburg & Putz, 2012), *SHELXTL* (Sheldrick, 2008) and *publCIF* (Westrip, 2010).

6. Synthesis and crystallization

A mixture of 2-oxo-1,2-dihydroquinoline-4-carboxylic acid (0.5 g, 2.6 mmol), K_2CO_3 (0.73 g, 5.29 mmol), 1-bromohexane (0.66 g, 4 mmol) and tetra-*n*-butylammonium bromide as catalyst in DMF (25 ml) was stirred at room temperature for 48 h. The solution was filtered by suction, and the solvent was removed under reduced pressure. The residue was chromatographed on a silica-gel column using hexane and ethyl acetate (*v*/*v*, 95/5) as eluents to afford (I). Single crystals were obtained by slow evaporation of an ethanolic solution.

7. Refinement

Crystal data, data collection and structure refinement details are summarized in Table 2. All H atoms were located in difference-Fourier maps and were refined freely.

Funding information

The support of NSF–MRI grant No. 1228232 for the purchase of the diffractometer and Tulane University for support of the Tulane Crystallography Laboratory are gratefully acknowledged.

References

Bolognesi, M. L., Cavalli, A., Valgimigli, L., Bartolini, M., Rosini, M., Andrisano, V., Recanatini, M. & Melchiorre, C. (2007). *J. Med. Chem.* **50**, 6446–6449.
Bouzian, Y., Faizi, M. S. H., Mague, J. T., Otmani, B. E., Dege, N., Karrouchi, K. & Essassi, E. M. (2019*a*). *Acta Cryst.* E**75**, 980–983.
Bouzian, Y., Karrouchi, K., Anouar, E. H., Bouhfid, R., Arshad, S. & Essassi, E. M. (2019*b*). *Acta Cryst.* E**75**, 912–916.
Brandenburg, K. & Putz, H. (2012). *DIAMOND*, Crystal Impact GbR, Bonn, Germany.
Bruker (2016). *APEX3* and *SAINT*. Bruker AXS, Inc., Madison, Wisconsin, USA.
Cannalire, R., Barreca, M. L., Manfroni, G. & Cecchetti, V. (2016). *J. Med. Chem.* **59**, 16–41.
Chu, X. M., Wang, C., Liu, W., Liang, L. L., Gong, K. K., Zhao, C. Y. & Sun, K. L. (2019). *Eur. J. Med. Chem.* **161**, 101–117.
Filali Baba, Y., Kandri Rodi, Y., Hayani, S., Jasinski, J. P., Kaur, M. & Essassi, E. M. (2017*a*). *IUCrData*, **2**, x170917.
Filali Baba, Y., Kandri Rodi, Y., Jasinski, J. P., Kaur, M., Ouzidan, Y. & Essassi, E. M. (2017*b*). *IUCrData*, **2**, x171072.
Filali Baba, Y., Mague, J. T., Kandri Rodi, Y., Ouzidan, Y., Essassi, E. M. & Zouihri, H. (2016). *IUCrData*, **1**, x160997.
Groom, C. R., Bruno, I. J., Lightfoot, M. P. & Ward, S. C. (2016). *Acta Cryst.* B**72**, 171–179.
Hu, Y. Q., Gao, C., Zhang, S., Xu, L., Xu, Z., Feng, L. S., Wu, X. & Zhao, F. (2017). *Eur. J. Med. Chem.* **139**, 22–47.
Krause, L., Herbst-Irmer, R., Sheldrick, G. M. & Stalke, D. (2015). *J. Appl. Cryst.* **48**, 3–10.
Palit, P., Paira, P., Hazra, A., Banerjee, S., Gupta, A. D., Dastidar, S. G. & Mondal, N. B. (2009). *Eur. J. Med. Chem.* **44**, 845–853.
Panda, S. S., Liaqat, S., Girgis, A. S., Samir, A., Hall, C. D. & Katritzky, A. R. (2015). *Bioorg. Med. Chem. Lett.* **25**, 3816–3821.
Paterna, R., André, V., Duarte, M. T., Veiros, L. F., Candeias, N. R. & Gois, P. M. P. (2013). *Eur. J. Org. Chem.* **2013**, 6280–6290.
Pinz, M., Reis, A. S., Duarte, V., da Rocha, M. J., Goldani, B. S., Alves, D., Savegnago, L., Luchese, C. & Wilhelm, E. A. (2016). *Eur. J. Pharmacol.* **780**, 122–128.
Sekgota, K. C., Majumder, S., Isaacs, M., Mnkandhla, D., Hoppe, H. C., Khanye, S. D., Kriel, F. H., Coates, J. & Kaye, P. T. (2017). *Bioorg. Chem.* **75**, 310–316.
Sheldrick, G. M. (2008). *Acta Cryst.* A**64**, 112–122.
Sheldrick, G. M. (2015*a*). *Acta Cryst.* A**71**, 3–8.
Sheldrick, G. M. (2015*b*). *Acta Cryst.* C**71**, 3–8.
Spackman, M. A. & Jayatilaka, D. (2009). *CrystEngComm*, **11**, 19–32.
Tang, Q. D., Duan, Y. L., Xiong, H. H., Chen, T., Xiao, Z., Wang, L. X., Xiao, Y. Y., Huang, S. M., Xiong, Y., Zhu, W., Gong, P. & Zheng, P. (2018). *Eur. J. Med. Chem.* **158**, 201–213.
Turner, M. J., MacKinnon, J. J., Wolff, S. K., Grimwood, D. J., Spackman, P. R., Jayatilaka, D. & Spackman, M. A. (2017). *CrystalExplorer17.5*. University of Western Australia. http://hirshfeldsurface.net.
Westrip, S. P. (2010). *J. Appl. Cryst.* **43**, 920–925.
Xu, Z., Gao, C., Ren, Q. C., Song, X. F., Feng, L. S. & Lv, Z. S. (2017). *Eur. J. Med. Chem.* **139**, 429–440.

supporting information

Acta Cryst. (2020). E**76**, 642-645 [https://doi.org/10.1107/S2056989020004521]

Crystal structure and Hirshfeld surface analysis of hexyl 1-hexyl-2-oxo-1,2-dihydroquinoline-4-carboxylate

Younos Bouzian, Sevgi Kansiz, Lhassane Mahi, Noureddine Hamou Ahabchane, Joel T. Mague, Necmi Dege, Khalid Karrouchi and El Mokhtar Essassi

Computing details

Data collection: *APEX3* (Bruker, 2016); cell refinement: *SAINT* (Bruker, 2016); data reduction: *SAINT* (Bruker, 2016); program(s) used to solve structure: *SHELXT/5* (Sheldrick, 2015*a*); program(s) used to refine structure: *SHELXL2018/3* (Sheldrick, 2015*b*); molecular graphics: *DIAMOND* (Brandenburg & Putz, 2012); software used to prepare material for publication: *SHELXTL* (Sheldrick, 2008) and *publCIF* (Westrip, 2010).

Hexyl 1-hexyl-2-oxo-1,2-dihydroquinoline-4-carboxylate

Crystal data

$C_{22}H_{31}NO_3$
M_r = 357.48
Monoclinic, $P2_1/c$
a = 17.6928 (7) Å
b = 13.2512 (5) Å
c = 8.5916 (3) Å
β = 90.184 (2)°
V = 2014.30 (13) Å^3
Z = 4
$F(000)$ = 776
D_x = 1.179 Mg m^{-3}
Cu $K\alpha$ radiation, λ = 1.54178 Å
Cell parameters from 9350 reflections
θ = 5.0–72.3°
μ = 0.61 mm^{-1}
T = 150 K
Block, colourless
0.25 × 0.17 × 0.10 mm

Data collection

Bruker D8 VENTURE PHOTON 100 CMOS diffractometer
Radiation source: INCOATEC IμS micro–focus source
Mirror monochromator
Detector resolution: 10.4167 pixels mm^{-1}
ω scans
Absorption correction: multi-scan (*SADABS*; Krause *et al.*, 2015)
T_{min} = 0.82, T_{max} = 0.94
14697 measured reflections
3924 independent reflections
3044 reflections with $I > 2\sigma(I)$
R_{int} = 0.048
θ_{max} = 72.4°, θ_{min} = 4.2°
h = −21→21
k = −16→15
l = −9→10

Refinement

Refinement on F^2
Least-squares matrix: full
$R[F^2 > 2\sigma(F^2)]$ = 0.046
$wR(F^2)$ = 0.105
S = 1.07
3924 reflections
359 parameters
0 restraints
Primary atom site location: dual
Secondary atom site location: difference Fourier map
Hydrogen site location: difference Fourier map
All H-atom parameters refined

$w = 1/[\sigma^2(F_o^2) + (0.028P)^2 + 0.8763P]$
where $P = (F_o^2 + 2F_c^2)/3$
$(\Delta/\sigma)_{max} < 0.001$

$\Delta\rho_{max} = 0.19$ e Å^{-3}
$\Delta\rho_{min} = -0.18$ e Å^{-3}

Special details

Geometry. All esds (except the esd in the dihedral angle between two l.s. planes) are estimated using the full covariance matrix. The cell esds are taken into account individually in the estimation of esds in distances, angles and torsion angles; correlations between esds in cell parameters are only used when they are defined by crystal symmetry. An approximate (isotropic) treatment of cell esds is used for estimating esds involving l.s. planes.

Refinement. Refinement of F^2 against ALL reflections. The weighted R-factor wR and goodness of fit S are based on F^2, conventional R-factors R are based on F, with F set to zero for negative F^2. The threshold expression of $F^2 > 2\text{sigma}(F^2)$ is used only for calculating R-factors(gt) etc. and is not relevant to the choice of reflections for refinement. R-factors based on F^2 are statistically about twice as large as those based on F, and R- factors based on ALL data will be even larger.

Fractional atomic coordinates and isotropic or equivalent isotropic displacement parameters (Å²)

	x	*y*	*z*	U_{iso}*/U_{eq}
O1	0.38830 (7)	0.40574 (9)	0.54321 (12)	0.0338 (3)
O2	0.68998 (7)	0.45106 (10)	0.80686 (14)	0.0384 (3)
O3	0.66596 (7)	0.37452 (8)	0.57906 (13)	0.0308 (3)
N1	0.40867 (8)	0.38809 (9)	0.80434 (14)	0.0254 (3)
C1	0.53672 (9)	0.37846 (11)	0.90859 (17)	0.0251 (3)
C2	0.58415 (10)	0.36524 (11)	1.03887 (19)	0.0281 (4)
H2	0.6393 (11)	0.3633 (14)	1.024 (2)	0.034 (5)*
C3	0.55465 (10)	0.35284 (12)	1.18543 (19)	0.0303 (4)
H3	0.5872 (10)	0.3427 (14)	1.279 (2)	0.039 (5)*
C4	0.47679 (10)	0.35250 (12)	1.20670 (18)	0.0298 (4)
H4	0.4558 (10)	0.3457 (14)	1.309 (2)	0.032 (5)*
C5	0.42866 (10)	0.36311 (12)	1.08128 (18)	0.0277 (4)
H5	0.3734 (10)	0.3620 (13)	1.098 (2)	0.031 (5)*
C6	0.45761 (9)	0.37626 (11)	0.93073 (17)	0.0246 (3)
C7	0.43350 (10)	0.39750 (11)	0.65289 (17)	0.0270 (3)
C8	0.51480 (10)	0.40045 (11)	0.63199 (18)	0.0269 (3)
H8	0.5319 (10)	0.4116 (14)	0.529 (2)	0.036 (5)*
C9	0.56382 (9)	0.39364 (11)	0.75165 (17)	0.0260 (3)
C10	0.32666 (10)	0.39452 (12)	0.83043 (19)	0.0285 (4)
H10A	0.3196 (10)	0.4370 (13)	0.927 (2)	0.029 (4)*
H10B	0.3059 (10)	0.4312 (14)	0.736 (2)	0.033 (5)*
C11	0.28830 (10)	0.29203 (12)	0.8470 (2)	0.0295 (4)
H11A	0.3155 (10)	0.2489 (14)	0.924 (2)	0.027 (4)*
H11B	0.2890 (10)	0.2551 (14)	0.742 (2)	0.035 (5)*
C12	0.20666 (10)	0.30564 (14)	0.8979 (2)	0.0351 (4)
H12A	0.2056 (11)	0.3463 (15)	1.001 (2)	0.046 (6)*
H12B	0.1785 (11)	0.3465 (16)	0.818 (2)	0.046 (6)*
C13	0.16396 (11)	0.20777 (15)	0.9228 (2)	0.0390 (4)
H13A	0.1920 (11)	0.1658 (16)	1.009 (2)	0.049 (6)*
H13B	0.1668 (11)	0.1653 (16)	0.826 (2)	0.045 (6)*
C14	0.08281 (12)	0.22432 (18)	0.9724 (3)	0.0485 (5)
H14A	0.0815 (13)	0.2635 (19)	1.075 (3)	0.070 (7)*

H14B	0.0564 (13)	0.2674 (19)	0.896 (3)	0.068 (7)*
C15	0.03901 (15)	0.1279 (2)	0.9986 (4)	0.0656 (7)
H15A	0.0625 (16)	0.085 (2)	1.085 (3)	0.086 (9)*
H15B	−0.0159 (16)	0.1416 (19)	1.031 (3)	0.076 (8)*
H15C	0.0378 (15)	0.089 (2)	0.895 (3)	0.086 (9)*
C16	0.64634 (10)	0.40936 (12)	0.71935 (18)	0.0280 (4)
C17	0.74124 (10)	0.40261 (14)	0.5285 (2)	0.0329 (4)
H17A	0.7783 (11)	0.3728 (14)	0.602 (2)	0.036 (5)*
H17B	0.7456 (11)	0.4763 (17)	0.533 (2)	0.044 (6)*
C18	0.75172 (10)	0.36435 (13)	0.3648 (2)	0.0325 (4)
H18A	0.7468 (11)	0.2897 (16)	0.365 (2)	0.046 (6)*
H18B	0.7102 (11)	0.3912 (14)	0.299 (2)	0.037 (5)*
C19	0.82624 (11)	0.39951 (15)	0.2953 (2)	0.0352 (4)
H19A	0.8683 (12)	0.3685 (16)	0.350 (2)	0.050 (6)*
H19B	0.8308 (11)	0.4748 (17)	0.311 (2)	0.049 (6)*
C20	0.83340 (11)	0.37729 (15)	0.1223 (2)	0.0385 (4)
H20A	0.8297 (12)	0.3045 (18)	0.106 (2)	0.052 (6)*
H20B	0.7894 (12)	0.4082 (16)	0.068 (2)	0.047 (6)*
C21	0.90568 (12)	0.41679 (18)	0.0503 (2)	0.0440 (5)
H21A	0.9504 (13)	0.3819 (17)	0.102 (3)	0.059 (7)*
H21B	0.9100 (14)	0.490 (2)	0.075 (3)	0.069 (7)*
C22	0.90816 (15)	0.4025 (2)	−0.1249 (3)	0.0579 (6)
H22A	0.9029 (15)	0.332 (2)	−0.154 (3)	0.080 (9)*
H22B	0.8651 (16)	0.439 (2)	−0.178 (3)	0.077 (8)*
H22C	0.9566 (14)	0.4306 (19)	−0.170 (3)	0.069 (7)*

Atomic displacement parameters (Å²)

	U^{11}	U^{22}	U^{33}	U^{12}	U^{13}	U^{23}
O1	0.0371 (7)	0.0385 (7)	0.0258 (6)	−0.0021 (5)	−0.0026 (5)	0.0022 (5)
O2	0.0351 (7)	0.0463 (7)	0.0337 (6)	−0.0085 (6)	0.0025 (5)	−0.0066 (5)
O3	0.0322 (7)	0.0304 (6)	0.0301 (6)	−0.0038 (5)	0.0069 (5)	−0.0041 (5)
N1	0.0296 (8)	0.0219 (6)	0.0248 (7)	−0.0008 (5)	0.0015 (5)	−0.0004 (5)
C1	0.0335 (9)	0.0164 (7)	0.0253 (8)	−0.0021 (6)	0.0003 (6)	−0.0015 (5)
C2	0.0324 (10)	0.0213 (7)	0.0307 (8)	−0.0010 (7)	−0.0018 (7)	−0.0003 (6)
C3	0.0402 (10)	0.0247 (8)	0.0260 (8)	−0.0032 (7)	−0.0036 (7)	0.0005 (6)
C4	0.0443 (11)	0.0228 (8)	0.0223 (8)	−0.0037 (7)	0.0036 (7)	−0.0014 (6)
C5	0.0352 (10)	0.0221 (7)	0.0259 (8)	−0.0025 (7)	0.0037 (7)	−0.0018 (6)
C6	0.0344 (9)	0.0166 (7)	0.0230 (7)	−0.0006 (6)	0.0006 (6)	−0.0009 (5)
C7	0.0363 (10)	0.0198 (7)	0.0249 (8)	−0.0010 (6)	0.0004 (7)	0.0009 (6)
C8	0.0346 (9)	0.0223 (8)	0.0240 (8)	−0.0023 (6)	0.0044 (7)	0.0001 (6)
C9	0.0336 (9)	0.0177 (7)	0.0267 (8)	−0.0012 (6)	0.0033 (7)	−0.0027 (6)
C10	0.0293 (9)	0.0266 (8)	0.0297 (8)	0.0024 (7)	0.0027 (7)	0.0014 (7)
C11	0.0302 (9)	0.0276 (8)	0.0308 (8)	−0.0008 (7)	0.0016 (7)	0.0002 (7)
C12	0.0316 (10)	0.0358 (9)	0.0380 (10)	0.0001 (7)	0.0033 (8)	0.0040 (8)
C13	0.0340 (10)	0.0405 (10)	0.0426 (10)	−0.0039 (8)	0.0017 (8)	0.0051 (8)
C14	0.0342 (11)	0.0584 (13)	0.0530 (13)	−0.0058 (10)	0.0038 (10)	0.0092 (10)
C15	0.0428 (14)	0.0811 (18)	0.0730 (18)	−0.0203 (13)	0.0015 (13)	0.0178 (15)

C16	0.0335 (9)	0.0224 (7)	0.0282 (8)	−0.0006 (7)	0.0025 (7)	−0.0001 (6)
C17	0.0296 (10)	0.0343 (10)	0.0347 (9)	−0.0024 (7)	0.0053 (7)	−0.0017 (7)
C18	0.0326 (10)	0.0319 (9)	0.0332 (9)	−0.0029 (7)	0.0027 (8)	−0.0019 (7)
C19	0.0304 (10)	0.0415 (10)	0.0336 (9)	−0.0011 (8)	0.0037 (8)	−0.0016 (7)
C20	0.0372 (11)	0.0432 (11)	0.0350 (10)	−0.0033 (8)	0.0038 (8)	−0.0031 (8)
C21	0.0374 (12)	0.0568 (13)	0.0379 (10)	−0.0043 (10)	0.0080 (9)	−0.0041 (9)
C22	0.0516 (15)	0.0812 (18)	0.0410 (12)	−0.0106 (13)	0.0126 (11)	−0.0032 (12)

Geometric parameters (Å, º)

O1—C7	1.2388 (19)	C12—H12A	1.04 (2)
O2—C16	1.2096 (19)	C12—H12B	1.01 (2)
O3—C16	1.3376 (19)	C13—C14	1.515 (3)
O3—C17	1.451 (2)	C13—H13A	1.05 (2)
N1—C7	1.380 (2)	C13—H13B	1.00 (2)
N1—C6	1.395 (2)	C14—C15	1.511 (3)
N1—C10	1.471 (2)	C14—H14A	1.02 (3)
C1—C2	1.408 (2)	C14—H14B	0.98 (3)
C1—C6	1.413 (2)	C15—H15A	1.02 (3)
C1—C9	1.447 (2)	C15—H15B	1.03 (3)
C2—C3	1.374 (2)	C15—H15C	1.02 (3)
C2—H2	0.985 (19)	C17—C18	1.507 (2)
C3—C4	1.390 (2)	C17—H17A	0.992 (19)
C3—H3	0.998 (19)	C17—H17B	0.98 (2)
C4—C5	1.378 (2)	C18—C19	1.522 (2)
C4—H4	0.956 (18)	C18—H18A	0.99 (2)
C5—C6	1.404 (2)	C18—H18B	0.99 (2)
C5—H5	0.988 (18)	C19—C20	1.521 (2)
C7—C8	1.451 (2)	C19—H19A	0.97 (2)
C8—C9	1.346 (2)	C19—H19B	1.01 (2)
C8—H8	0.945 (19)	C20—C21	1.515 (3)
C9—C16	1.502 (2)	C20—H20A	0.98 (2)
C10—C11	1.525 (2)	C20—H20B	0.99 (2)
C10—H10A	1.011 (18)	C21—C22	1.518 (3)
C10—H10B	1.015 (18)	C21—H21A	1.02 (2)
C11—C12	1.521 (2)	C21—H21B	1.00 (3)
C11—H11A	0.997 (17)	C22—H22A	0.97 (3)
C11—H11B	1.022 (18)	C22—H22B	1.01 (3)
C12—C13	1.516 (3)	C22—H22C	1.01 (3)
C16—O3—C17	115.00 (13)	C12—C13—H13B	109.7 (12)
C7—N1—C6	123.04 (14)	H13A—C13—H13B	105.0 (16)
C7—N1—C10	117.09 (13)	C15—C14—C13	114.0 (2)
C6—N1—C10	119.84 (13)	C15—C14—H14A	106.8 (14)
C2—C1—C6	118.59 (14)	C13—C14—H14A	109.8 (14)
C2—C1—C9	124.05 (15)	C15—C14—H14B	110.3 (14)
C6—C1—C9	117.37 (14)	C13—C14—H14B	110.2 (14)
C3—C2—C1	121.07 (16)	H14A—C14—H14B	105 (2)

C3—C2—H2	119.7 (11)	C14—C15—H15A	111.5 (16)
C1—C2—H2	119.3 (11)	C14—C15—H15B	112.2 (15)
C2—C3—C4	120.01 (16)	H15A—C15—H15B	106 (2)
C2—C3—H3	122.4 (11)	C14—C15—H15C	107.7 (16)
C4—C3—H3	117.5 (11)	H15A—C15—H15C	111 (2)
C5—C4—C3	120.45 (16)	H15B—C15—H15C	108 (2)
C5—C4—H4	118.9 (11)	O2—C16—O3	123.42 (15)
C3—C4—H4	120.6 (11)	O2—C16—C9	124.59 (15)
C4—C5—C6	120.45 (16)	O3—C16—C9	111.96 (13)
C4—C5—H5	119.7 (10)	O3—C17—C18	108.01 (14)
C6—C5—H5	119.9 (10)	O3—C17—H17A	108.2 (11)
N1—C6—C5	120.25 (15)	C18—C17—H17A	112.2 (11)
N1—C6—C1	120.34 (14)	O3—C17—H17B	108.5 (12)
C5—C6—C1	119.41 (14)	C18—C17—H17B	111.1 (11)
O1—C7—N1	121.22 (15)	H17A—C17—H17B	108.8 (16)
O1—C7—C8	122.79 (15)	C17—C18—C19	111.86 (15)
N1—C7—C8	115.96 (14)	C17—C18—H18A	108.8 (11)
C9—C8—C7	122.71 (15)	C19—C18—H18A	112.4 (12)
C9—C8—H8	121.0 (11)	C17—C18—H18B	108.6 (11)
C7—C8—H8	116.2 (11)	C19—C18—H18B	107.9 (11)
C8—C9—C1	120.44 (15)	H18A—C18—H18B	107.1 (15)
C8—C9—C16	118.29 (14)	C20—C19—C18	113.51 (15)
C1—C9—C16	121.13 (14)	C20—C19—H19A	109.0 (12)
N1—C10—C11	113.70 (13)	C18—C19—H19A	110.2 (12)
N1—C10—H10A	106.4 (10)	C20—C19—H19B	108.3 (11)
C11—C10—H10A	111.3 (10)	C18—C19—H19B	108.6 (12)
N1—C10—H10B	105.1 (10)	H19A—C19—H19B	107.0 (17)
C11—C10—H10B	110.0 (10)	C21—C20—C19	113.87 (16)
H10A—C10—H10B	110.2 (14)	C21—C20—H20A	109.8 (13)
C12—C11—C10	110.15 (14)	C19—C20—H20A	109.0 (12)
C12—C11—H11A	109.5 (10)	C21—C20—H20B	109.1 (12)
C10—C11—H11A	111.0 (10)	C19—C20—H20B	108.0 (12)
C12—C11—H11B	108.9 (10)	H20A—C20—H20B	106.7 (17)
C10—C11—H11B	109.7 (11)	C20—C21—C22	112.87 (18)
H11A—C11—H11B	107.6 (14)	C20—C21—H21A	108.7 (13)
C13—C12—C11	114.40 (15)	C22—C21—H21A	110.7 (13)
C13—C12—H12A	108.3 (11)	C20—C21—H21B	108.2 (14)
C11—C12—H12A	109.1 (11)	C22—C21—H21B	109.4 (14)
C13—C12—H12B	108.1 (12)	H21A—C21—H21B	106.7 (19)
C11—C12—H12B	109.7 (12)	C21—C22—H22A	112.0 (16)
H12A—C12—H12B	107.0 (16)	C21—C22—H22B	111.1 (15)
C14—C13—C12	112.89 (17)	H22A—C22—H22B	106 (2)
C14—C13—H13A	109.1 (11)	C21—C22—H22C	111.1 (14)
C12—C13—H13A	108.5 (11)	H22A—C22—H22C	110 (2)
C14—C13—H13B	111.3 (12)	H22B—C22—H22C	107 (2)

C6—C1—C2—C3	−1.6 (2)	C7—C8—C9—C16	−173.12 (13)
C9—C1—C2—C3	178.89 (14)	C2—C1—C9—C8	176.52 (15)

C1—C2—C3—C4	0.5 (2)	C6—C1—C9—C8	−3.0 (2)
C2—C3—C4—C5	0.9 (2)	C2—C1—C9—C16	−7.8 (2)
C3—C4—C5—C6	−1.2 (2)	C6—C1—C9—C16	172.65 (13)
C7—N1—C6—C5	−177.49 (14)	C7—N1—C10—C11	99.07 (16)
C10—N1—C6—C5	4.7 (2)	C6—N1—C10—C11	−82.96 (17)
C7—N1—C6—C1	3.2 (2)	N1—C10—C11—C12	171.38 (14)
C10—N1—C6—C1	−174.68 (13)	C10—C11—C12—C13	−178.17 (15)
C4—C5—C6—N1	−179.30 (14)	C11—C12—C13—C14	−179.66 (16)
C4—C5—C6—C1	0.1 (2)	C12—C13—C14—C15	−179.8 (2)
C2—C1—C6—N1	−179.37 (13)	C17—O3—C16—O2	−8.3 (2)
C9—C1—C6—N1	0.2 (2)	C17—O3—C16—C9	169.68 (13)
C2—C1—C6—C5	1.3 (2)	C8—C9—C16—O2	143.61 (17)
C9—C1—C6—C5	−179.14 (13)	C1—C9—C16—O2	−32.2 (2)
C6—N1—C7—O1	178.45 (14)	C8—C9—C16—O3	−34.38 (19)
C10—N1—C7—O1	−3.6 (2)	C1—C9—C16—O3	149.83 (14)
C6—N1—C7—C8	−3.5 (2)	C16—O3—C17—C18	−175.71 (14)
C10—N1—C7—C8	174.39 (13)	O3—C17—C18—C19	174.17 (14)
O1—C7—C8—C9	178.56 (15)	C17—C18—C19—C20	−170.54 (17)
N1—C7—C8—C9	0.6 (2)	C18—C19—C20—C21	177.03 (17)
C7—C8—C9—C1	2.7 (2)	C19—C20—C21—C22	−174.6 (2)

Hydrogen-bond geometry (Å, º)

D—H···*A*	*D*—H	H···*A*	*D*···*A*	*D*—H···*A*
C4—H4···O1^{i}	0.960 (17)	2.475 (17)	3.3670 (19)	154.7 (15)

Symmetry code: (i) *x*, *y*, *z*+1.